This paper describes objective technical results and analysis. Any subjective views or opinions that might be expressed in the paper do not necessarily represent the views of the U.S. Department of Energy or the United States Government.

SAND2021-7332C

Analysis of Grid Support Functionality Dynamics Under Ride-Through Requirements Using Power-Hardware-in-the-Loop Implementation

Edgardo Desarden-Carrero[1], Rachid Darbali-Zamora[2], Erick E. Aponte-Bezares[1]

[1]University of Puerto Rico-Mayagüez, Mayagüez, Puerto Rico 00682, USA
[2]Sandia National Laboratories, Albuquerque, New Mexico, 87185, USA

***Abstract* – Due to the increased penetration in Distributed Energy Resources (DERs), especially in Photovoltaic (PV) systems, voltage and frequency regulation has become a topic of interest. Utilities have been requesting DER voltage and frequency support for almost two decades. Their request was addressed by standards such as the IEEE Std 1547-2018. With the continuous improvements in inverters' ability to control their output voltage, power, and frequency, a group of advanced techniques to support the grid is now required by the interconnection standard. These techniques are known as Grid Support Functions (GSF), and they allow the inverter to provide voltage and frequency support to the grid as well as the ability to ride-through abnormal events. Understanding how a GSF behaves is challenging, especially when multiple GSFs are combined to help the utility to control the system voltage and frequency. This paper evaluates the effects of GSF's on the IEEE Std 1547.1-2020 Unintentional Islanding Test 5B by comparing simulation results from a developed PV inverter model and experimental results from a Power Hardware-in-the-Loop platform.**

Index Terms – photovoltaic inverter, grid support functions, ride-through, Power-Hardware-in-the-Loop.

I. Introduction

Grid Support Functions (GSF) are advanced modes of operation that allow Photovoltaic (PV) inverters to provide support to the grid under abnormal voltage and frequency conditions. GSFs provide a benefit to both grid voltage and frequency stability while at the same time reducing the need of costly grid upgrades [1], [2]. However, GSFs can cause deviation in voltage and frequency during ride-through operations [3]. Also, variation in voltage and frequency during the ride-through process can make islanding detection more difficult for PV inverters. As a result, the Unintentional Islanding (UI) detection time can be longer or undetectable in some cases [4], [5]. The IEEE Std 1547.1-2020 Cat. B UI test requires PV inverters to operate in combinations of different GSFs in a variety of modes of operation to test PV inverter UI detection performance under different conditions [6], [7], [8].

II. Reactive Power Modes

Reactive power support can provide grid voltage stability. Multiple reactive power modes are mandatory in IEEE Std 1547-2020. The reactive power mode can be set to Constant Power Factor (CPF), Volt-Var Control (VVC), Watt-Var Control (WVC), and Constant Reactive Power (CQ) [2]. Only VVC and WVC can be set to their default settings or aggressive mode. The continuous adjustment of active and reactive power depending on the voltage, frequency, and active power in the Point of Common Coupling (PCC) can lead the system to voltage and frequency oscillations that could exceed the PV inverter tripping point setting. The IEEE Std 1547-2020 requires a unity constant power factor mode to be the default settings of any installed PV inverter until the electric power source operator specifies different conditions [6].

A. Constant Power Factor (CPF)

The CPF mode sets the PV inverter to operates at the same level of real and reactive power delivered. This is independent of the amount of energy supplied by the PV inverter [9]. The maximum allowable response time for the equipment under test to maintain constant power is 10 s or less [7].

B. Constant Reactive Power (CQ)

In the CQ mode, the PV inverter must maintain constant reactive power no matter what has been specified (injection or absorption mode) by the utility operator [6]. The CQ mode lacks accuracy for voltage regulation and in some cases tends to unnecessary reactive power absorption [10], [11].

C. Volt-Var Control (VVC)

The VVC allows a PV inverter to provide reactive power based on the PCC's voltage measurements [12]. Thus, a VVC is a relationship between voltage and reactive power. PV inverters can absorb or inject reactive power to improve voltage stability [13], [14]. The voltage stability is achieved by either utilizing excess capacity not being used for real power or reducing real power and allowing reactive power generation. **Error! Reference source not found.** shows the VVC characteristic curve as a linear function that controls the reactive output power based on the PV inverter's voltage.

D. Active Power-Reactive Power Control (WVC)

The WVC dynamic power reference mode is another technology that achieves voltage regulation [15]. In this mode, the PV inverter controls the reactive power output dynamically as a function of active power. **Error! Reference source not found.** shows the WVC characteristic curve for the UI Test. This test has two modes of operation: Default (DFLT) and Most Aggressive (MA).

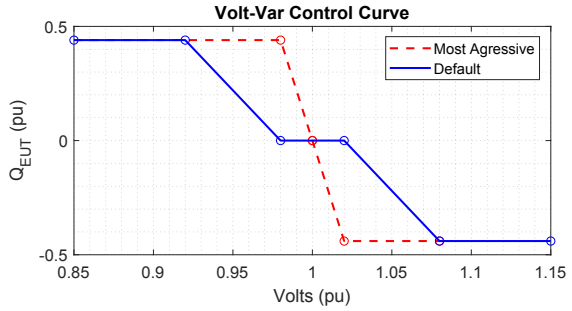

Sandia National Laboratories is a multimission laboratory managed and operated by National Technology & Engineering Solutions of Sandia, LLC, a wholly owned subsidiary of Honeywell International Inc., for the U.S. Department of Energy's National Nuclear Security Administration under contract DE-NA0003525.

Fig. 1. Volt-Var Control Characteristic Curve.

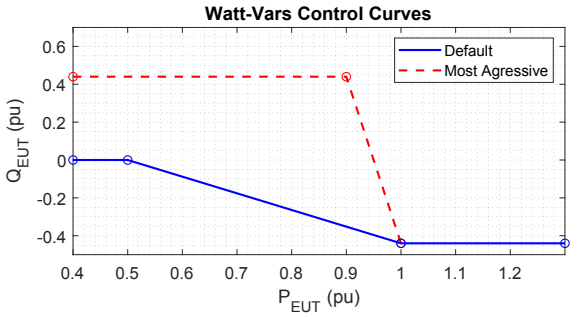

Fig. 2. Watt-Vars Control Characteristic Curve.

III. Active Power Modes

The active power mode uses the grid voltage and frequency information to generate an active power reference for the PV inverter [6]. These active power techniques have been designed to facilitate the high integration of DERs. This mode has two options available: Volt-Watt Control (VWC) and Frequency-Watt Control (FWC) [7].

A. Volt-Watt Control Mode (VWC)

In the VWC, the input for the control is the grid voltage, and the control action is the active power reference from the VWC function [16]. **Error! Reference source not found.** shows the VWC power characteristic curve for the UI test.

B. Frequency-Watt Control Mode (FWC)

In the Frequency-Watt Control (FWC), the control input is the grid frequency, and the control action is the active power, as shown in **Error! Reference source not found.**. In this function, the inverter's active power is controlled based on a Frequency-Watt droop function that causes the inverter to share a portion of the load change, thereby supporting the grid [17], [18].

IV. Ride-Through Scenario

Due to the increase in DER penetration levels, many utilities depend on PV systems to maintain grid stability. The IEEE Std 1547-2018 specifies the mandatory, uniform, and universal requirements at the PCC when interconnecting a PV inverter to the grid. The IEEE Std 1547-2108 requires an island detection disconnecting time of less than 2 s but now requires mandatory ride-through operation for PV inverters with that capability. The mandatory procedure specifies that PV inverters must stay connected and actively regulate voltage and frequency at the PCC, riding through abnormal voltage and frequency conditions [19].

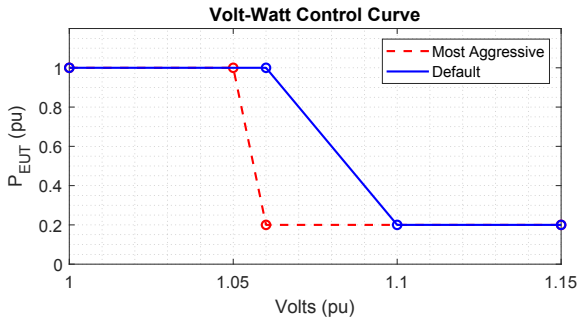

Fig. 3: Volt-Watt Control Characteristic Curve

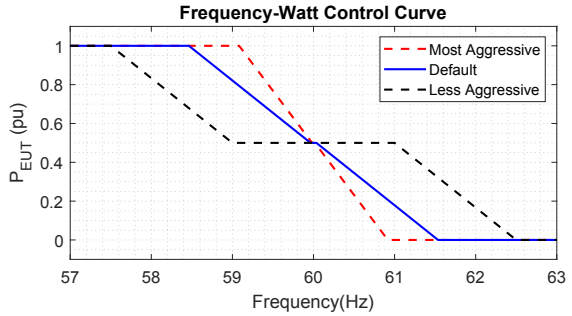

Fig. 4. Frequency-Watt Control Characteristic Curve.

To effectively regulate voltage and frequency at the PCC, the PV inverter depends on GSFs. GSFs can be combined to allow a PV inverter to control both voltage and frequency at its PCC. The GSFs response time can also be adjusted in different aggressiveness mode levels; Less Aggressive (LA), DFLT, and MA. Response time is defined as the duration for the PV inverter to increase or decrease its output power from 0% to 90%. The IEEE P1547 UI Test specifies the response times as 10 s for LA, 5 s, and 10 s for DFLT, and 1 s for MA. **Error! Reference source not found.** shows a PV inverter's active power adjusted in LA, DFLT, and MA modes. PV inverters at different GSFs aggressiveness levels can support the utility under abnormal voltage and frequency situations. However, when PV inverters are connected to a high fluctuating bus, special considerations must be given when setting GSFs at MA. The high voltage and current fluctuation in the bus combined with GSFs at MA can push PV inverters to exceed its tripping limits, causing them to disconnect or to go into momentary cessation. This condition could represent more instability to the system due sudden increase in the load.

V. Implementing Grid Support Functions

Different approaches can be implemented to enable PV inverters with GSF control. An effective method to implement GSF control is by using the control tables specified by the IEEE in **Error! Reference source not found.** through **Error! Reference source not found.** to help set the trigger points in the controller depending on the GSF implemented. Once the controller is triggered, it will begin to increase or decrease the active or reactive power based on the controlled variable in the control curve. The response time in which the output power will be increased or decreased will be specified with the mode of operation (LA, DFLT, MA), as shown in **Error! Reference**

source not found.. Many inverter manufacturers rely on using ramps to control the inverter's output power through GSFs.

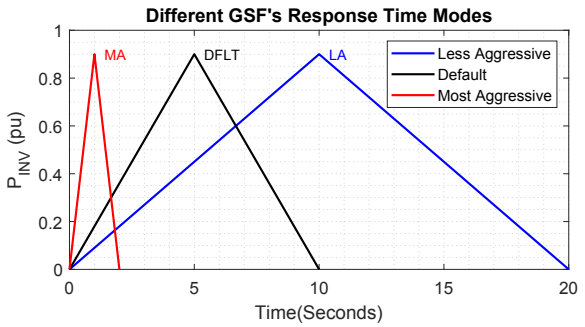

Fig. 5. Different Response Times as Specified in the IEEE Std 1547.1

In order to implement this concept in a simulation tool, it is necessary to sample and capture the time duration produced by the control ramp. The ramp slope will be controlled with a gain block, and the output power will be accumulated and stored, as shown in **Error! Reference source not found.**.

VI. Test Scenario with Power-Hardware-in-the-Loop

There are guides and parameters of operation specified by the IEEE to develop a GSF model, but there is no specific approach to mathematically represent them. An approach is to model the system using GSFs regulation and compare the results with experimental results obtained from testing commercially available devices. When similar behavior is achieved, it is possible to optimize the GSF control of the model.

Results for the IEEE Std 1547.1 UI Test 5B are obtained for a commercially available PV inverter using a Power-Hardware-in-the-Loop (PHIL) platform [20], [21]. The PV inverter is tested operating with GSFs (VVC, FWC and VWC set to DFLT) [22]. In test 5 the PV inverter is connected to the grid in parallel with a RLC load. The parallel RLC load is intended to absorb the entire PV inverter capacity with active power and nonreactive power.

Test 5B is performed in the three different modes (DFLT, LA, MA) to assess the control performance of the GSFs in different scenarios. An unbalanced reactive power of (a total of 2.3 kVars and 767 Vars per phase) is added to the load to recreate the same initial conditions of Test 5B performed with PHIL platform. This initial unbalance will also force the GSFs to start operating immediately after de islanded condition is created at 1 s. The IEEE standard specifies that UI tests implemented with PHIL techniques should be sustained for at least 10 s in island mode with the inverter UI detection option disabled. The developed model must comply with the exact requirement of time to be reliable. Implementing a GSF is necessary to have a PV inverter model that operates similar to commercially available PV inverters, regulating voltage and current when islanded. One alternative in developing a PV inverter model is to use the Simulink dynamic load model.

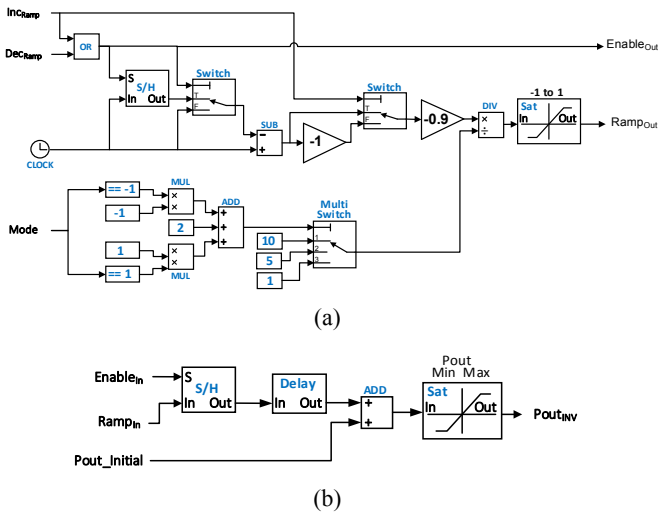

Fig. 6. Simulink Output Power and Ramp Control. (a) Increment and Decrement Ramp. (b) Memory to Hold Accumulated Power.

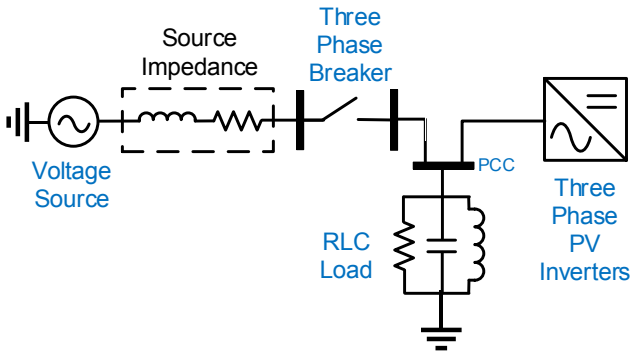

Fig. 7. Model of the Unintentional Islanding Test.

In order for the dynamic load model to operate as a power source, the active and reactive power setpoint are defined as negative values. The dynamic load is designed to regulate voltage, current, power, and frequency when connected at the PCC during the islanding test. It is important to note that the dynamic load model only operates as a power source and does not include islanding detection or the ability to execute UI disconnection. The model of the UI test is illustrated in Fig. 7.

VII. Power-Hardware-in-the-Loop GSF Validation

This test has been performed in a PHIL system with a commercially available PV inverter. The PV inverter was operated with the GSFs of VVC, FWC, and VWC in the DFLT mode.

The GSFs control parameters in DFLT were the following:

FWC:F <=59.96 Hz => Increase P | F > 60.036 Hz => Decrease P
VVC: V_L<=271 V => Increase Q | V_L >= 282 V => Decrease Q
VWC:V_L>=293 V => Decrease P

The GSF response time was as follows:

FWC: 0.9/5 Pout_pu/s
VVC: 0.9/10 Qout_pu/s
VWC: 0.9/10 Qout_pu/s

The UI detection and mitigation option in the inverter was set to "OFF".

In order to control the system's voltage and frequency response, the PV inverter operates at a specified deadband. When the parameters are outside their respective deadband, the system controls one variable at a time. **Error! Reference source not found.** shows the results for IEEE Std 1547.1 test 5B in DFLT mode implemented with PHIL. Voltage and frequency deadbands are shown with dashed horizontal lines (identified in the same color as the waveforms scale). Notice that the settings for the frequency deadband force the frequency waveform to operate at 60 Hz.

The test illustrated in **Error! Reference source not found.** demonstrates that the PV inverter has been initially programmed to only supply active power without supplying any reactive power. However, these two quantities will change as the GSFs take control. The parallel RLC load absorbs the full PV inverter capacity as active power (24 kW Total, 8 kW per phase). The RLC load's reactive power is not ideally tunned in resonance. This means the utility is supplying reactive power (a total of 2.3 kVars and 767 Vars per phase) to compensate.

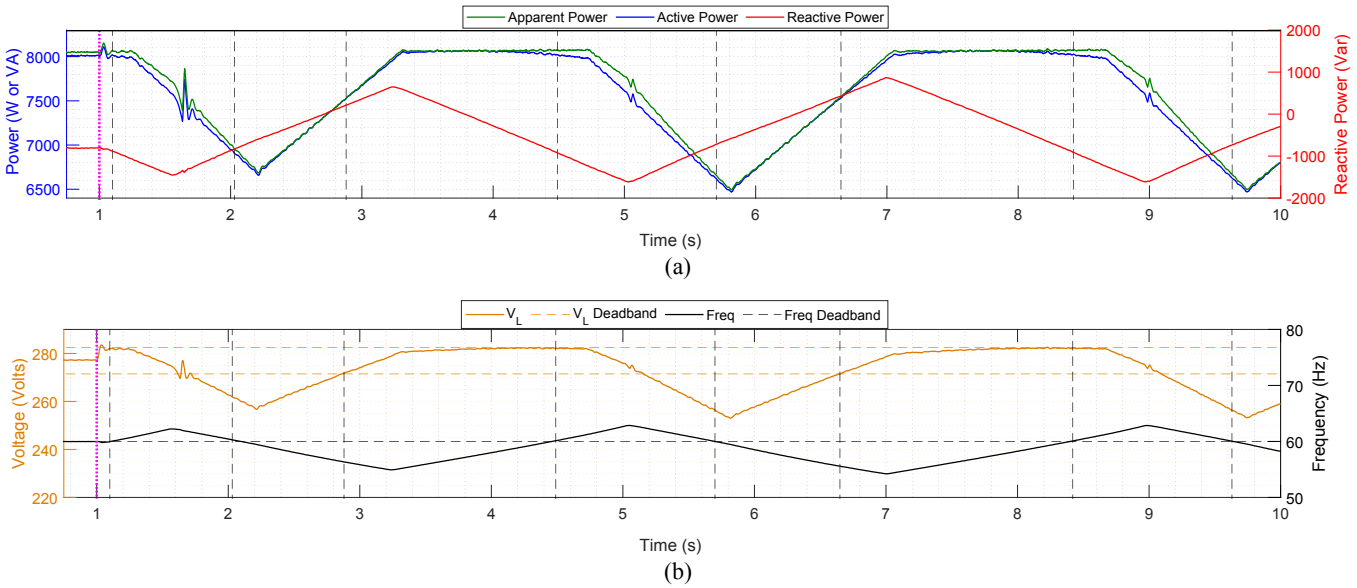

Fig. 8. IEEE Std 1547 UI Cat B. Test 5B Implemented with PHIL (VVC, FWC and VWC). (a) Power at Load. (b) Load Voltage and Frequency.

The supplied reactive power provided by the utility will act as an unbalance initial condition that the GSFs will try to regulate into the control deadbands after the system is islanded after 1 s. The islanded signal is shown as a dotted magenta vertical line in 1 s. **Error! Reference source not found.** (b) shows that after 1 s, the system is islanded and the frequency value is outside the deadband. From 1 s to 2.1 s, the system is able to control the frequency. At 2.1 s the frequency returns into the deadband, and the frequency control stops. At this point, the voltage parameter is outside the deadband. From 2.1 s to 2.9 s, the system controls the voltage and regulates it into the deadband at 2.9 s. Table I summarizes the PV inverter GSF control throughout the test period.

TABLE I:
ENABLED GRID SUPPORT FUNCTION CONTROL SETTINGS

Start Time (s)	End Time (s)	Enabled Control
2.9	4.5	Frequency
4.5	5.6	Frequency
5.6	6.6	Voltage
6.6	8.3	Frequency
8.3	9.5	Frequency
9.5	10.0	Voltage

Notice that when the frequency control is repeated at small time period, both parameters are in control. Due to the restricted frequency range, the system returns to frequency control immediately. At 4 s and 7.8 s, when the system's active power is almost equal to the system's apparent power, the reactive power is close to zero due to the PV inverter operating at maximum capacity. When the frequency changes from increasing to decreasing, the voltage is at the lower limit of the deadband, and a spike in signals is observed, caused by the activation of the VVC. With these plots showing the behavior of power, voltage, and frequency in test 5B when implemented with PHIL techniques, it is possible to develop a simulation model with GSF control.

VIII. MATLAB/SIMULINK MODEL RESULTS

A. IEEE Std 1547.1 Cat B UI Test 5B (Mode: DFLT)

Error! Reference source not found. shows the results of test 5 implemented in Simulink. Notice that there are similarities when comparing **Error! Reference source not found.** with the results from **Error! Reference source not found.**. Two more plots were added to analyze the behavior and performance of GSFs. Fig. 9 (c), indicates when the system has

enabled voltage control or frequency control, and Fig. 9 (d) illustrates how the system manages the real and the reactive power. This is an indicator that the designed GSFs are operating as desired.

In **Error! Reference source not found.** (b), when the model goes into an islanded state after 1 s, the amount of reactive power supplied by the utility should be handled by the PV inverter. To fulfill test 5B, the amount of reactive power provided by the PV inverter should be zero. The PV inverter achieves this requirement by increasing the frequency achieve a resonance state which forces the demanded reactive power to zero. The load frequency is incremented by the PV inverter from 60 Hz to 62 Hz to reach resonant state. From the results shown in **Error! Reference source not found.** (a), at 1.1 s, the resonance effect can be observed when the reactive power reaches zero after the island condition at 1 s.

Immediately after the island condition in 1 s, the frequency increases. It can be observed in **Error! Reference source not found.** (c) and **Error! Reference source not found.** (d) that the FWC is activated when the frequency control signal is too high, indicating the frequency needs to be modified. As shown in

Error! Reference source not found. (d), from 1 s to 1.8 s, the FWC starts reducing the active power and increasing the reactive power to reduce the frequency to its nominal levels. A reduction in active power will cause the system voltage to decrease. Decreasing the system voltage will cause a reduction in the reactive power at the load. Therefore, the PV inverter will reduce the system frequency to match the drop in reactive power. At 1.7 s the frequency returns to its nominal value, but the voltage moves outside the deadband.

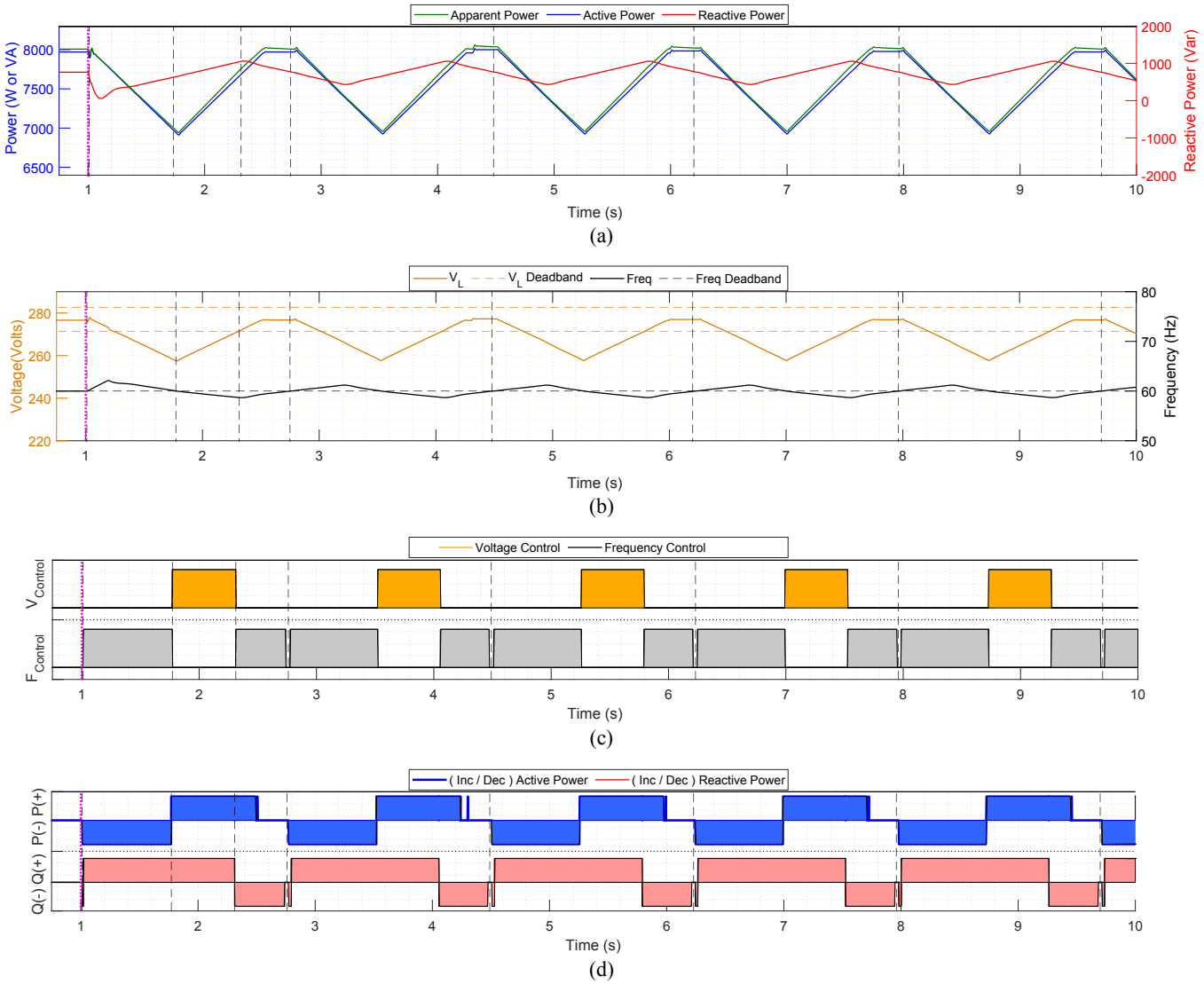

Fig. 9. IEEE Std 1547 UI Cat B. Test 5B Implemented with MATLAB/Simulink (VVC, FWC and VWC set to DFLT). (a) Power at Load. (b) Load Voltage and Frequency. (c) Control Areas. (d) Inverter Output Power Levels.

As a result, the voltage control indicator becomes 1, which means the system voltage needs to be adjusted, as shown in Fig. 9 (c). Results from **Error! Reference source not found.** (d) illustrate that The VVC starts increasing the active and

reactive power at 1.7 s until the system voltage returns to the control deadband area at 2.3 s.

When the VVC increases the reactive power, the system voltage increases as well, and the system frequency decrease to match reactive power. This reduction in frequency will trigger the FWC at 2.3 s, increasing the active power, and decreasing the reactive power increase the system frequency. At 2.5 s the system still needs to increase the frequency, but the PV inverter is approaching its maximum capacity. The FWC sets the active power to zero at 2.5 s to avoid an overload condition but decreases the reactive power to achieve the frequency deadband at 2.7 s. After this point, the GSFs repeat the same behavior every 1.78 s. Test 5B in DFLT mode never increases the system voltage over 293 V or 1.06 pu. For this reason, the VWC illustrated in **Error! Reference source not found.** never activates during this test.

B. IEEE Std 1547.1 Cat B UI Test 5B (Mode: LA)

The LA mode operates at the slowest response time. This mode tends to be a stable control because of its wider deadbands and longer response time. The following parameters are used to test the PV inverter in the LA mode:

The GSFs control parameters in LA were the following:

FWC: F <=59.00 Hz => Increase P | F > 61.00 Hz => Decrease P
VVC: V_L <=271 V => Increase Q | V_L >= 282 V => Decrease Q
VWC: V_L >=293 V => Decrease P

The GSF response time was as follows:

FWC: 0.9/10 Pout_pu/s
VVC: 0.9/10 Qout_pu/s
VWC: 0.9/10 Pout_pu/s

Error! Reference source not found. illustrates the results obtained for the LA case. Notice from **Error! Reference source not found.** (b) that after the island is formed at 1 s, both parameters, voltage, and frequency were in control inside their respective deadbands.

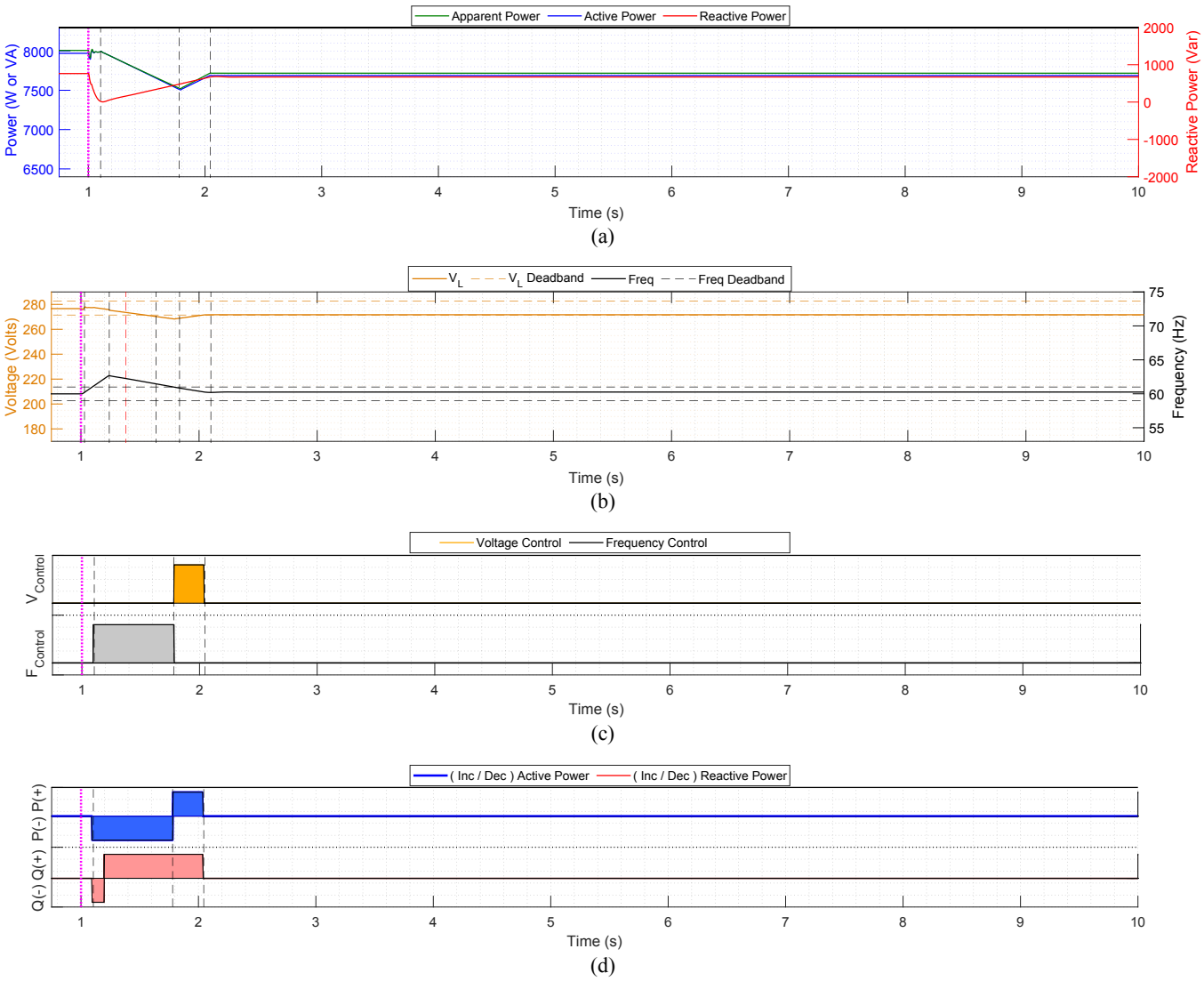

Fig. 10. IEEE Std 1547 UI Cat B. Test 5B Implemented with MATLAB/Simulink (VVC, FWC and VWC set to LA). (a) Power at Load. (b) Load Voltage and Frequency. (c) Control Areas. (d) Inverter Output Power Levels.

Error! Reference source not found. shows the results for the LA mode. Notice in **Error! Reference source not found.** (b) that after the island is formed at 1 s, both voltage and frequency were in control inside their respective deadbands. At 1.1 s the frequency goes out its deadband, and the system performs a frequency control procedure until 1.6 s. At 1.6 s the voltage is outside of its deadband and the VVC performs a voltage control operation until 1.7 s. Notice that the system reaches a stable state at 1.7 s; after that point, the system remains in a stable state until reaching 10 s. As illustrated in **Error! Reference source not found.** (b), the wide range in the voltage deadbands (10 V range) in combination with the wide range in the frequency deadband (2 Hz range) produces a wider equilibrium area for the GSFs controls.

C. IEEE Std 1547.1 Cat B UI Test 5B (Mode: MA)

When the GSF is set to MA mode, it represents the most challenging scenario to maintain the PV inverter operating in a stable state. The challenge for PV inverters is to attempt to maintain voltage and frequency under normal conditions adjusting the real and the reactive power within 1 s of reaction time. Stability in the MA mode dramatically depends on the load when the PV inverter is islanded. When the PV inverter is connected to the grid, the PV inverter operates stable due to the grids stiffness and support. However, a significant oversight in detecting an island condition arises when the PV inverter is operating, providing support to the grid through ride-through actions and GSFs. The following parameters are used to test the PV inverter performance in the MA mode:

The GSFs control parameters in MA were the following:

FWC: F <= 59.98 Hz => Increase P | F >60.02 Hz => Decrease P
VVC: V_L < 277 V => Increase Q | V_L > 277 V => Decrease Q
VWC: V_L >= 290 V => Decrease P

The GSF response time was as follows:

FWC: 0.9/1 Pout_pu/s

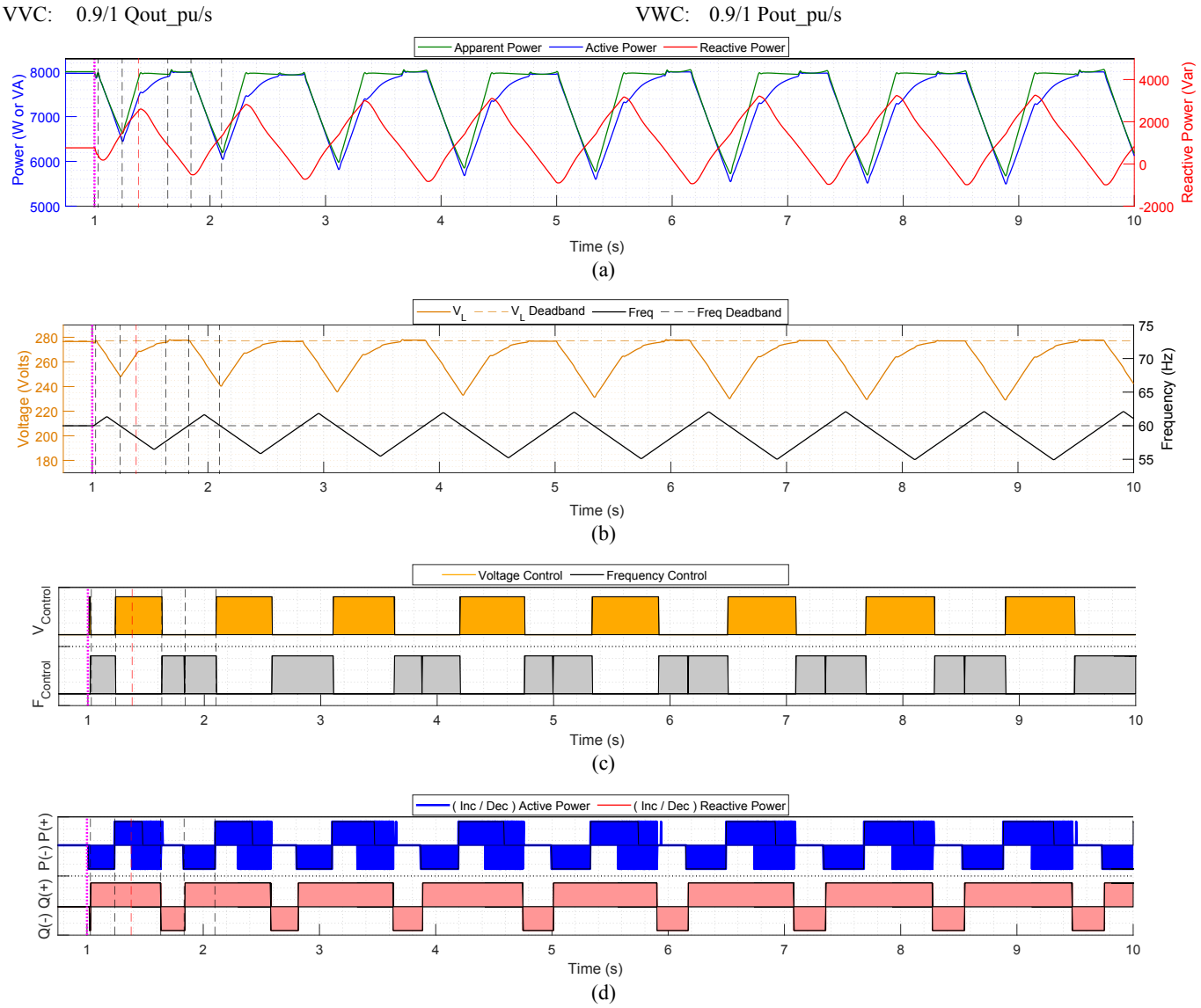

Fig. 11. IEEE Std 1547 UI Cat B. Test 5B Implemented with MATLAB/Simulink (VVC, FWC and VWC set to MA). (a) Power at Load. (b) Load Voltage and Frequency. (c) Control Areas. (d) Inverter Output Power Levels.

Error! Reference source not found. illustrates the results obtained for the MA case scenario. Notice from the results **Error! Reference source not found.** (a) through **Error! Reference source not found.** (d) that there is noticeably shorter response times for this mode of operation. This rapid control scheme, in combination with an RLC load that is not in perfect balanced resonance, demonstrates that the system has considerably more oscillations.

The results presented in **Error! Reference source not found.** (c) illustrate that there is a pattern of three control areas that are repeating every 0.8 s. This short time in the pattern repetition reflects a stabilized system even though it could have larger oscillations. **Error! Reference source not found.** (a) illustrates that there's an average of 4 kVars of oscillations in this mode of operation. Also, these results demonstrate that the active power is reduced from 8 kW to 5.5 kW. This considerable oscillation in power is reflected in significant voltage and frequency variations. The terminal voltage illustrates a drop of 40 V while the frequency magnitudes vary 5 Hz from the nominal 60 Hz.

IX. Conclusion

IEEE Std 1547.1 stipulates the requirements for the GSFs operation, but there is not a specific technique or approach to implement GSFs for a PV inverter. This paper evaluates GSF's effects on the IEEE Std 1547.1-2020 UI Test 5B implemented using a PHIL platform. Using a simulation model of a PV inverter with programed GSFs a comparison between simulated and experimental results is illustrated. A simulation model with different GSFs is programmed and implemented to represent and help study the effect of GSFs in the stabilization of voltage and frequency in distribution systems. Also, the simulation model is able to test how GSFs impact the islanding detection in PV inverters. This model provides an understanding into

GSFs operations as well as insight into PV inverter control dynamics for maintaining voltage and frequency stability. PHIL results illustrate how the PV inverter is able to both inject and absorb both active and reactive power to regulate voltage and frequency.

ACKNOWLEDGMENT

Sandia National Laboratories is a multi-mission laboratory managed and operated by National Technology and Engineering Solutions of Sandia, LLC., a wholly-owned subsidiary of Honeywell International, Inc., for the US Department of Energy's National Nuclear Security Administration under contract DE-NA-0003525.

This work was sponsored in part by the Consortium for Hybrid Resilient Energy Systems (CHRES) under grant number DE-NA0003982 from the National Nuclear Security Administration part of the U.S. Department of Energy.

REFERENCES

[1] Institute of Electrical and Electronics Engineers, "IEEE 1547.1-2020 Standard Conformance Test Interconnecting Distributed Energy," 2020.

[2] N. Gökmen, W. Hu, and Z. Chen, "A Simple PV Inverter Power Factor Control Method Based on Solar Irradiance Variation", *2017 IEEE Manchester PowerTech*, 2017.

[3] S. Gonzalez, E. Desarden-Carrero, N. S. Gurule and E. E. Aponte-Bezares, "Unintentional Islanding Evaluation Utilizing Discrete RLC Circuit Versus Power Hardware-in-the Loop Method", *2019 IEEE 46th Photovoltaic Specialists Conference (PVSC)*, 2019, pp. 1-8.

[4] E. Desardén-Carrero, R. Darbali-Zamora and E. E. Aponte-Bezares, "Analysis of Commonly Used Local Anti-Islanding Protection Methods in Photovoltaic Systems in Light of the New IEEE 1547-2018 Standard Requirements", *2019 IEEE 46th Photovoltaic Specialists Conference (PVSC)*, 2019, pp. 2962-2969.

[5] M. Ropp, D. Schultz, J. Neely and S. Gonzalez, "Effect of Grid Support Functions and VRT/FRT Capability on Autonomous Anti-Islanding Schemes in Photovoltaic Converters", *2016 IEEE 43rd Photovoltaic Specialists Conference (PVSC)*, 2016, pp. 1853-1856.

[6] Institute of Electrical and Electronics Engineers, "IEEE Std 1547-2018 (Revision of IEEE Std 1547-2003) : IEEE Standard for Interconnection and Interoperability of Distributed Energy Resources with Associated Electric Power Systems Interfaces.," IEEE, 2018.

[7] Institute of Electrical and Electronics Engineers, "P1547.1/D9.5 Draft Standard Conformance Test Procedures for Equipment Interconnecting Distributed Energy Resources with Electric Power Systems and Associated Interfaces", 2019.

[8] E. Desarden-Carrero, R. Darbali-Zamora, N. S. Gurule, E. Aponte-Bezares and S. Gonzalez, "Evaluation of the IEEE Std 1547.1-2020 Unintentional Islanding Test Using Power Hardware-in-the-Loop", *2020 47th IEEE Photovoltaic Specialists Conference (PVSC)*, 2020, pp. 2262-2269.

[9] J. Seuss, M. J. Reno, R. J. Broderick, and S. Grijalva, "SANDIA REPORT Analysis of PV Advanced Inverter Functions and Setpoints under Time Series Simulation," 2016.

[10] B. Craciun, D. Sera, E. A. Man, T. Kerekes, V. A. Muresan and R. Teodorescu, "Improved Voltage Regulation Strategies by PV Inverters in LV Rural Networks", *2012 3rd IEEE International Symposium on Power Electronics for Distributed Generation Systems (PEDG)*, 2012, pp. 775-781.

[11] J. Johnson, A. Summers, R. Darbali-Zamora, J. Hernandez-Alvidrez, J. Quiroz, D. Arnold, J. Anandan; "Distribution Voltage Regulation Using Extremum Seeking Control with Power Hardware-in-the-Loop," *IEEE Journal of Photovoltaics*, vol. 8, no. 6, pp. 1824-1832, Nov. 2018.

[12] A. Alkuhayli, F. Hafiz and I. Husain, "Volt/Var Control in Distribution Networks with High Penetration of PV Considering Inverter Utilization", *2017 IEEE Power & Energy Society General Meeting*, 2017, pp. 1-5.

[13] M. G. Kashani, M. Mobarrez and S. Bhattacharya, "Smart Inverter Volt-Watt Control Design in High PV Penetrated Distribution Systems", *2017 IEEE Energy Conversion Congress and Exposition (ECCE)*, 2017, pp. 4447-4452.

[14] F. Ding, A. Nguyen, S. Walinga, A. Nagarajan, M. Baggu, S. Chakraborty, M. McCarty and F. Bell, "Application of Autonomous Smart Inverter Volt-VAR Function for Voltage Reduction Energy Savings and Power Quality in Electric Distribution Systems", *2017 IEEE Power & Energy Society Innovative Smart Grid Technologies Conference (ISGT)*, 2017, pp. 1-5.

[15] Y. Liu, W. Qin, L. Dq, D. Q. J. Lqj, D. Q. J. Lei, and F. Li, "Distribution Network Voltage Control by Active Power/Reactive Power Injection from PV Inverters", *2018 13th IEEE Conference on Industrial Electronics and Applications (ICIEA)*, 2018, pp. 543-547.

[16] K. Prabakar, M. Shirazi, A. Singh and S. Chakraborty, "Advanced Photovoltaic Inverter Control Development and Validation in a Controller-Hardware-in-the-Loop Test Bed", *2017 IEEE Energy Conversion Congress and Exposition (ECCE)*, 2017, pp. 1673-1679.

[17] D. Pattabiraman, R. H. Lasseter. and T. M. Jahns, "Comparison of Grid Following and Grid Forming Control for a High Inverter Penetration Power System", *2018 IEEE Power & Energy Society General Meeting (PESGM)*, 2018, pp. 1-5.

[18] R. Darbali-Zamora, J. E. Quiroz, J. Hernández-Alvidrez, J. Johnson and E. I. Ortiz-Rivera, "Validation of a Real-Time Power Hardware-in-the-Loop Distribution Circuit Simulation with Renewable Energy Sources," *2018 IEEE 7th World Conference on Photovoltaic Energy Conversion (WCPEC) (A Joint Conference of 45th IEEE PVSC, 28th PVSEC & 34th EU PVSEC)*, 2018, pp. 1380-1385.

[19] J. Johnson, J. C. Neely, J. J. Delhotal and M. Lave, "Photovoltaic Frequency–Watt Curve Design for Frequency Regulation and Fast Contingency Reserves", *IEEE Journal of Photovoltaics*, vol. 6, no. 6, pp. 1611-1618, Nov. 2016.

[20] R. Darbali-Zamora, J. Johnson, N. S. Gurule, M. J. Reno, N. Ninad and E. Apablaza-Arancibia, "Evaluation of Photovoltaic Inverters Under Balanced and Unbalanced Voltage Phase Angle Jump Conditions", *2020 47th IEEE Photovoltaic Specialists Conference (PVSC)*, 2020, pp. 1562-1569.

[21] R. Darbali-Zamora, J. Hernandez-Alvidrez, A. Summers, N. S. Gurule, M. J. Reno and J. Johnson, "Distribution Feeder Fault Comparison Utilizing a Real-Time Power Hardware-in-the-Loop Approach for Photovoltaic System Applications", *2019 IEEE 46th Photovoltaic Specialists Conference (PVSC)*, 2019, pp. 2916-2922.

[22] N. Ninad *et al*., "PV Inverter Grid Support Function Assessment using Open-Source IEEE P1547.1 Test Package," *2020 47th IEEE Photovoltaic Specialists Conference (PVSC)*, 2020, pp.

1138-1144.